Applied Catalysis A: General 484 (2014) 33–38

Contents lists available at ScienceDirect

Applied Catalysis A: General

journal homepage: www.elsevier.com/locate/apcata

Surfactant-assisted synthesis of MgO: Characterization and catalytic activity on the transesterification of dimethyl carbonate with glycerol

Fidelis Stefanus Hubertson Simanjuntak[a], Seung Rok Lim[b], Byoung Sung Ahn[a], Hoon Sik Kim[b], Hyunjoo Lee[a,*]

[a] Clean Energy Research Center, Korea Institute of Science and Technology, 39-1 Hawolgok-dong, Sungbuk-gu, Seoul 136-791, Republic of Korea
[b] Department of Chemistry and Basic Research Institute of Science, Kyung Hee University, 1 Hoegi-dong, Dongdamun-gu, Seoul, Republic of Korea

ARTICLE INFO

Article history:
Received 15 March 2014
Received in revised form 12 June 2014
Accepted 29 June 2014
Available online 5 July 2014

Keywords:
Glycerol
Dimethyl carbonate
Glycerol carbonate
Magnesium oxide
Surfactant

ABSTRACT

Various forms of MgO were synthesized and used as catalysts in the transesterification of dimethyl carbonate (DMC) with glycerol for the synthesis of glycerol carbonate (GLC). MgO synthesized using a surfactant (a triblock copolymer of ethylene oxide/propylene oxide/ethylene oxide, known as Pluronic F127) showed a much higher GLC yield of 75.4% compared to other MgO catalysts synthesized without using a surfactant at reaction conditions of 90 °C, DMC/glycerol = 2, and catalyst/glycerol = 5 wt%. With an increase of the weight ratio of the surfactant/Mg precursor, the catalytic activity was increased. However, the activity did not change substantially when the surfactant/Mg precursor ratio was greater than 5. The high catalytic activity of MgO prepared with the surfactant (MgO–S) is attributed to the higher basic site concentration on the surface. This originated from low-coordination oxide ions at the corner sites (O_{3c}^{2-}), as shown in the basic site titration and UV–diffuse reflectance analysis results. It is also noted that MgO–S could be easily recovered after the reaction and reused at least five times without serious catalyst deactivation.

1. Introduction

Magnesium oxide (MgO) has long received attention for its applications in various fields as catalyst, adsorbent, semiconductor, paints, etc [1–5]. As a catalyst and a catalyst support, MgO has been used in various reactions such as oxidative dehydrogenation of butane, dehydrohalogenation, biodiesel production, dry reforming, etc [6–9]. Conventionally, MgO is synthesized from the thermal decomposition of various magnesium precursor [10,11]. To increase its catalytic activity, a number of other preparation methods have been studied, including precipitation, sol–gel, hydro/solvo thermal, vapor deposition, aerogel and hard-templating strategies, to fabricate MgO particles with various morphologies and/or porous structures [12–17].

Surfactant-assisted synthesis of MgO has also widely carried out to control its morphology, particle size, crystallinity and surface area, and thereby increase the absorption property and catalytic activity of MgO. Various forms of MgO have been synthesized using poly(4-styrenesulfonate) (PSS), triblock copolymer P123 ($PEO_{20}PPO_{70}PEO_{20}$), polyehtylene glycol (PEG), cetyltrimethylammonium bromide (CTAB), and dioctylsulfosuccinate sodium (AOT) as structure-directing agents to increase the surface area, pore volume, and pore size, and the adsorption capacity to phosphate, CO_2 and azo dye pollutants such as Congo red has thereby been increased [18–20,5].

Increasing surface area results in an increase of the surface basic site concentration, which facilitates the base catalyzed reaction. Jeon et al. prepared a MgO catalyst via a sol–gel process with the addition of poly(dimethylsiloxane-ethylene oxide) (PDMS-PEO) and reported that the prepared MgO exhibited a highly porous particle structure with higher surface area and basic site density. Thus, PDMS-PEO-assisted synthesized MgO showed enhanced catalytic activity compared to non-templated MgO in the production of biodiesel from canola oil [21]. Ganguly et al. synthesized nanoparticles of MgO with high surface area using CTAB and used them as a heterogeneous catalyst in Claisen–Schmidt condensation for the synthesis of chalcone [22].

Glycerol carbonate (GLC) is one of valuable glycerol derivative due to its potential for application as a membrane component for gas separation, as a component of coatings and detergents, and as a monomer of polycarbonate and polyurethane [23–27]. Among the various ways to synthesize GLC, the reaction of dimethyl

* Corresponding author. Tel.: +82 2 958 5868; fax: +82 2 958 5809.
E-mail address: hjlee@kist.re.kr (H. Lee).

http://dx.doi.org/10.1016/j.apcata.2014.06.028
0926-860X/

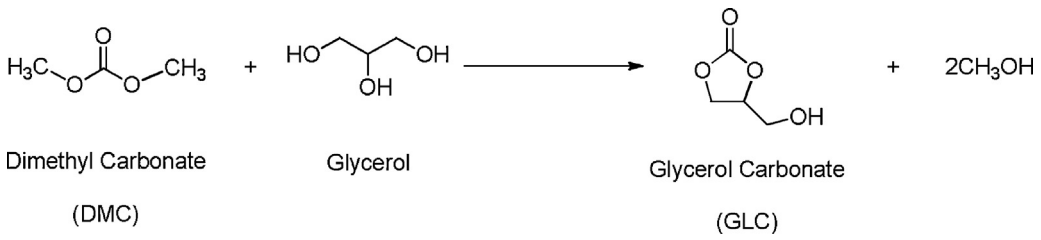

Scheme 1. Synthesis of glycerol carbonate (GLC) from glycerol and dimethyl carbonate (DMC).

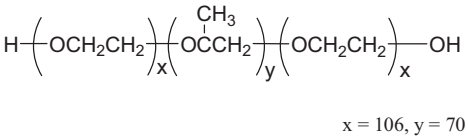

Fig. 1. Structure of surfactant, Pluronic F127.

carbonate (DMC) with glycerol is preferable in terms of mild reaction conditions and high glycerol carbonate yield (Scheme 1).

In the synthesis of glycerol carbonate from glycerol and DMC, a heterogeneous catalyst is preferred due to the high boiling temperature of glycerol and glycerol carbonate. Accordingly, various heterogeneous base catalysts including MgO, Mg—Al hydrotalcite, Mg—La mixed oxide, and Mg/Al/Zr have been studied [28–30]. Among them, as shown in Table S1, commercial MgO was found to have very poor catalytic activity compared to other Mg-based mixed oxide catalysts.

As a way to increase the catalytic activity of MgO, we synthesized MgO using a surfactant, pluronic F127 (Fig. 1), a triblock copolymer of ethylene oxide/propylene oxide/ethylene oxide. The morphology, surface area, and catalytic activity were compared with those of other MgO catalysts synthesized without using a surfactant. To elucidate the high catalytic activity of MgO prepared using the surfactant, the catalysts were analyzed using XRD, BET, and UV–vis. The basic site concentration of the catalyst was determined by the titration method and CO_2–TPD.

2. Experimental procedure

2.1. Catalyst preparation

All reagents were purchased from Sigma Aldrich and used as received without further purifications.

In this study, three kinds of magnesium oxide were synthesized: direct calcinations of $Mg(NO_3)_2{\cdot}6H_2O$ (MgO–C), precipitation of $Mg(NO_3)_2{\cdot}6H_2O$ using KOH (MgO–P) and calcination of $Mg(NO_3)_2{\cdot}6H_2O$—surfactant mixture (MgO–S).

In direct calcinations method, $Mg(NO_3)_2{\cdot}6H_2O$ was calcined at 680 °C in air atmosphere for 4 h.

In precipitation method, KOH (0.1 mol) in 50 g of distilled water was dropwised into the solution of $Mg(NO_3)_2{\cdot}6H_2O$ (6.6 g in 50 g of water) until the pH reached 10 and stirred for 24 h at room temperature. Formed white solid was filtered and washed with water, dried at 100 °C for 12 h, and subsequently calcined at 680 °C for 4 h.

In surfactant method, 12.8 g of triblock polymer, poly(ethylene oxide)-*b*-poly(propylene oxide)-*b*-poly(ethylene oxide), Pluronic F127 ($EO_{106}PO_{70}EO_{106}$) in 25 g of ethanol was stirred with $Mg(NO_3)_2{\cdot}6H_2O$ (2.56 g) and HNO_3 (0.49 g, 70 wt%). The mixture was stirred for 1 day at room temperature, then dried at 130 °C for 1 day. The solid was collected and calcined at 680 °C for 4 h in air. MgO catalyst were marked as MgO–S(10), MgO–S(5), MgO–S(1), MgO–S(0.5), and MgO–S(0.2) for samples prepared with surfactant/Mg precursor weight ratio of 10/1, 5/1, 1/1, 0.5/1, and 0.2/1, respectively.

2.2. Transesterification of DMC with glycerol

In typical reaction condition, glycerol (21.7 mmol, 2.0 g), DMC (43.4 mmol, 3.9 g) and magnesium oxide (0.1 g) were added to the 100 mL round-bottomed flask having reflux condenser. The mixture was heated with stirring at a desired temperature using bath oil. After the reaction, the catalyst was separated from the reaction mixture using syringe filter. The product was analyzed using HPLC (Waters) equipped with an Aminex HPX-87H column (Biorad) and a RI detector (Waters 410). The mobile phase used was a 5 mM H_2SO_4 aqueous solution and the flow rate was set at 0.6 mL/min.

2.3. Instrument

Structural characterizations of all samples were conducted using by X-Ray diffraction (Shimadzu XRD-6000, Japan). The Brunauer–Emmett–Teller (BET) surface area was determined using a Belsorp-mini II apparatus (BEL Inc., Osaka, Japan). Basic site concentration on the surface of catalyst was measured by benzoic acid titration method using Hammett indicators and TPD of CO_2. The titration was conducted three times and the average value was used in this report. The TPD experiment conducted using Belcat-B (Belcat, Osaka, Japan) equipped with a thermal conductivity detector (TCD). All samples were pretreated in situ in a He flow of 30 mL/min at 300 °C and exposed to a flowing mixture 3% of CO_2 in He for 10 min at 30 °C. Then, purged with He to remove physically adsorbed CO_2 and heated to 700 °C with heating rate 10 °C/min.

The UV–DRS (diffuse reflectance spectra) was obtained using a UV–vis–NIR infrared spectrophotometer (Cary 5000, Varian, USA). The particle shape image was measured using SEM (FEI Inc., Nova-Nano 200, Hillsboro).

3. Results and discussion

3.1. Effects of preparation method

Three kinds of magnesium oxides were prepared by calcining a magnesium precursor. MgO–C was obtained from the direct calcination of $Mg(NO_3)_2{\cdot}6H_2O$, while MgO–P was synthesized by calcining the precipitated magnesium precursor from $Mg(NO_3)_2{\cdot}6H_2O$ in a KOH solution. The third sample, MgO–S(5), was obtained by calcining a magnesium precursor that was obtained from a mixture of $Mg(NO_3)_2{\cdot}6H_2O$ and the surfactant Pluronic F127 ($EO_{106}PO_{70}EO_{106}$) with a weight ratio of surfactant/Mg precursor of 5.

The XRD patterns of the catalysts, shown in Fig. 2, revealed that all samples had a clear MgO crystalline phase. The crystallite size of MgO particles obtained from the Scherrer equation using the (2 0 0) peak was estimated to be 25.3, 10.7, and 14.0 nm for MgO–C, MgO–P, and MgO–S(5), respectively.

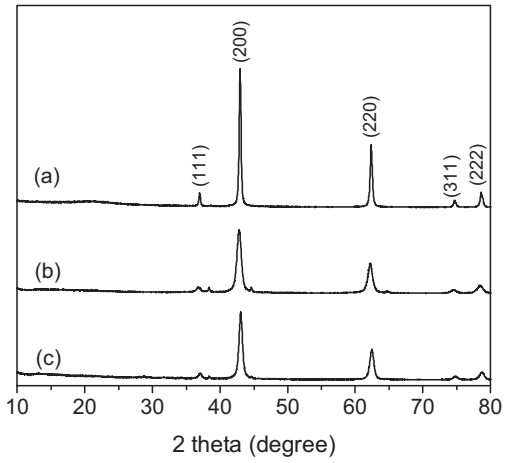

Fig. 2. XRD patterns of (a) MgO–C, (b) MgO–P, and (c) MgO–S(5).

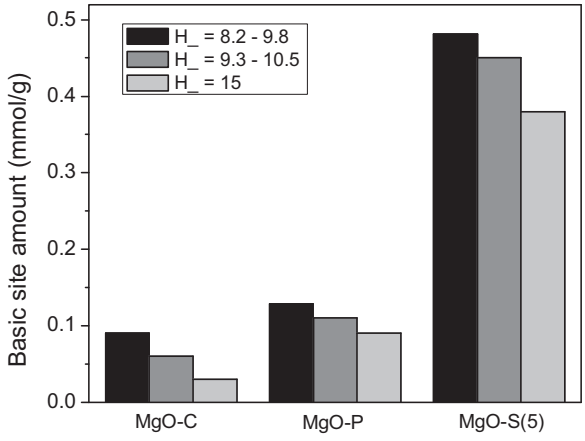

Fig. 4. Concentration of basic site on various MgO.

Table 1
Catalytic activities and surface areas of various MgO.

Catalyst	Catalytic activity			Surface area (m^2/g)
	Conversion of glycerol (%)	Yield of GLC (%)	Selectivity to GLC (%)	
MgO–C	12.0	11.1	92.5	5
MgO–P	17.8	16.0	89.8	104
MgO–S(5)	76.3	75.4	98.8	47

Reaction condition: DMC/glycerol = 2, catalyst/glycerol = 5 wt%, T = 90 °C, t = 30 min.

Using the prepared MgO as a catalyst, transesterification of DMC with glycerol for the synthesis of glycerol carbonate was conducted. The reaction was performed at 90 °C for 30 min with a DMC/glycerol molar ratio of 2 and a catalyst/glycerol weight ratio of 0.05. Table 1 shows MgO–S(5) have the highest yield of GLC, 75.4%, while MgO–C showed the lowest, 11.1%. In the case of MgO–P, the catalytic activity was very similar to that of MgO–C. The catalytic activity of MgO–S(5) is equal to or greater than those of other heterogeneous catalyst reported (see Table S1 in Supporting information). To elucidate these differences in catalytic activity with respect to the preparation methods, the surface area of the catalyst was measured.

Interestingly, as shown in Table 1, the catalytic activity and the surface area appeared to be irrelevant. The surface area of MgO–C and MgO–P, which have poor catalytic activity, was 5 m^2/g and 104 m^2/g, respectively, while the surface area of the more active MgO–S(5) was 47 m^2/g. SEM images of the prepared catalysts in Fig. 3 show that these catalysts have different morphologies. MgO–C is characterized by large flake-like shapes, while MgO–P is composed of much smaller irregular particles. In the case of MgO–S(5), it comprises small sphere-like particle.

To understand the catalytic activity of MgO according to the preparation method, the basic site strength and concentration of the prepared catalyst were measured by titrating the catalyst with a benzoic acid solution in the presence of a Hammett indicator, phenolphthalein (base strength H_- = 8.2–9.8), thymolpthalein (H_- = 9.3–10.5), 2,4 dinitroaniline (H_- = 15.0).

Fig. 4 shows that MgO–S(5) has a basic site concentration of 0.48 mmol/g ($H_- \geq 9.8$). Furthermore, highly basic sites ($H_- \geq 15$) were found in a concentration of 0.38 mmol/g. In contrast, the basic site concentrations ($H_- \geq 9.8$) of MgO–C and MgO–P were 0.09 and 0.13 mmol/g, respectively.

Additionally, CO_2–TPD experiments were conducted to investigate the basic site concentration and properties. As shown in Fig. 5, CO_2 desorption was detected in the broad temperature range of 100–650 °C at CO_2–TPD of MgO–S(5), indicating that MgO–S(5) has a weak basic sites (20–160 °C desorption) corresponding to lattice-bound OH groups, medium basic sites (160–400 °C desorption) corresponding to oxygen in the Mg^{2+} and O^{2-} pair, and strong basic sites (>400 °C desorption) corresponding to isolated O^{2-} [20]. Whereas, MgO–C and MgO–P were found to have weak and medium basic sites, respectively. Basic site concentration calculated from the TPD profile revealed that MgO–S(5) has the highest total basic site concentration of 0.39 mmol/g, followed by MgO–P and MgO–C with 0.14 and 0.04 mmol/g, respectively (Table S2 in Supporting information). These values are similar with the total basic sites concentration obtained from the titration method.

It was reported that the presence of low-coordination oxide ions at the corner (O_{3c}^{2-}) and the edge (O_{4c}^{2-}) sites plays a key role in the high catalytic activity of magnesium oxide in the Claisen–Schmidt condensation [31]. It was also reported that the

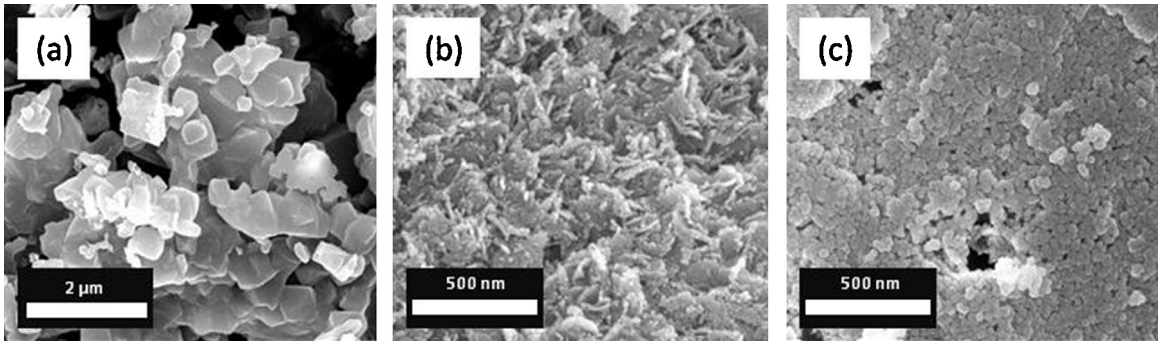

Fig. 3. SEM images of (a) MgO–C, (b) MgO–P and (c) MgO–S(5).

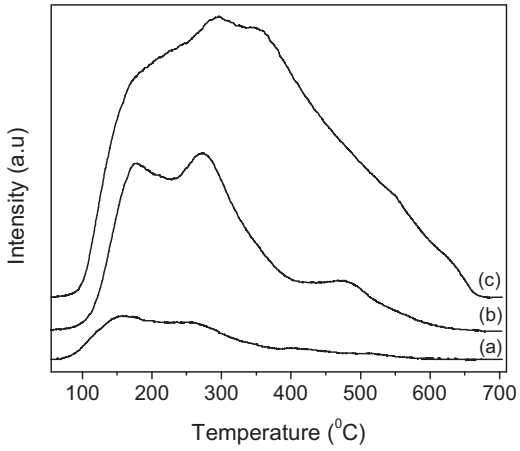

Fig. 5. TPD–CO_2 profiles for (a) MgO–C, (b) MgO–P, (c) MgO–S(5).

presence of low coordination sites gives rise to a specific optical transition in the UV light range, which could be measured using the UV–diffuse reflectance spectrum (UV–DRS) [32]. To detect the highly basic low-coordination oxide ion, although the presence of O^{2-} species in MgO–S(5) was observed from the CO_2–TPD experiment, UV–DRS of MgO–P and MgO–S(5) was measured. As shown in Fig. 6, in the spectrum of MgO–P, typical absorption peaks for MgO were detected at 270 nm (4.6 eV) and 215 nm (5.7 eV) with a low intensity, and these peaks correspond to surface excitons exerted by the low-coordination corner ($O_{3c}{}^{2-}$) and the edge ($O_{4c}{}^{2-}$) site ions [31,33]. Whereas, the UV–DRS of MgO–S(5) showed a stronger absorption peak at a range of 260–320 nm centered at about 282 nm (4.4 eV).

Although the cause of different maximum absorption energy is not clear, from the CO_2–TPD and UV–DRS experiments, it could be assumed that MgO–S(5) possess higher surface O^{2-} species compared to MgO–P. The higher O^{2-} concentration on MgO–S(5) surface compare to that of MgO–C and MgO–P, respectively, is ascribed to the use of the surfactant in the synthesis procedure. That is, during the preparation step of MgO–S(5), the basic oxygen site in the ether group of the surfactant Pluronic F127 binds to the Lewis acidic magnesium (Mg^{2+}) ion, thereby stabilizing the magnesium aqueous solution. Subsequently, during the calcination step, the surfactant is burned and removed from the catalyst system, which could result in the formation of numerous vacancies on the surface magnesium oxide, where low-coordination oxide O^{2-} exists.

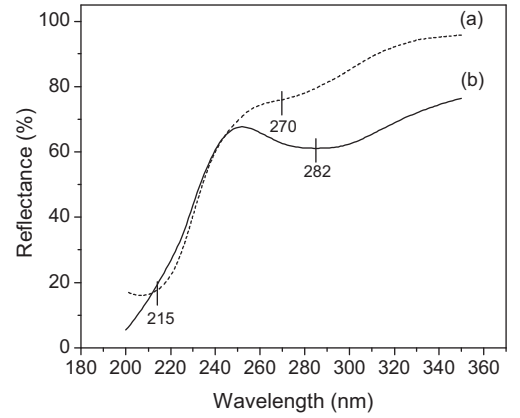

Fig. 6. UV–DRS (diffuse reflectance spectra) of (a) MgO–P and (b) MgO–S(5).

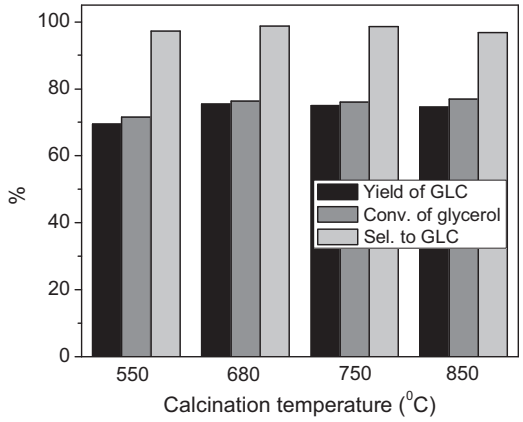

Fig. 7. Effect of calcination temperature on the catalytic activity of MgO–S(5).

3.2. Effect of calcination temperature

The effect of calcination temperature on the catalytic activity was investigated. MgO–P and MgO–S(5) were calcined at 550, 680, 750, and 850 °C and the results are shown in Fig. 7 and Fig. S1. As shown in Fig. 7, it was observed that increasing the calcination temperature from 550 to 680 °C resulted in a slight increase of GLC yield from 69.4 to 75.4% in the case of MgO–S(5). Further increase of temperature to 750 and 850 °C resulted in very similar GLC yields of 74.6 and 76.0%, indicating that calcination at temperature range of 680–850 °C did not have a noticeable impact on the catalytic activity. The catalytic activities of MgO–P and MgO–C with increased calcination temperature also revealed that the calcination temperature is not a decisive factor with respect to the catalytic activity of MgO–P and MgO–C (See Fig. S1 in Supporting information).

3.3. Effect of surfactant/Mg precursor ratio

To investigate the effect of surfactant amount, five different kinds of MgO were prepared using different surfactant/Mg precursor weight ratios of 10/1 (MgO–S(10)), 5/1 (MgO–S(5)), 1/1 (MgO–S(1)), 0.5/1 (MgO–S(0.5)), and 0.2/1 (MgO–S(0.2)). Fig. 8 shows that MgO–S(10) and MgO–S(5), which were made using large amounts of surfactant, exhibited higher catalytic activity for GLC than the catalysts made using a smaller amount of surfactant. The catalytic activity of MgO–S(0.2) was similar to that of MgO–P.

As discussed earlier, the use of the surfactant appeared to affect the basic site formation on the MgO. Fig. 9 shows that with an increase of the amount of surfactant used, the basic site

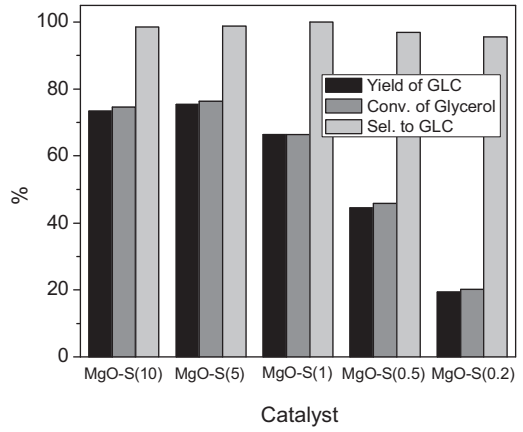

Fig. 8. Effect of surfactant/Mg precursor ratio on the catalytic activity of MgO–S. Reaction condition: DMC/glycerol = 2, catalyst/glycerol = 5 wt%, T = 90 °C, t = 30 min.

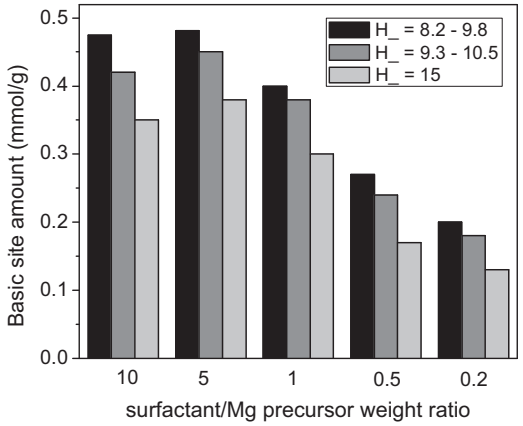

Fig. 9. Effect of surfactant/Mg precursor ratio on the basic site concentration.

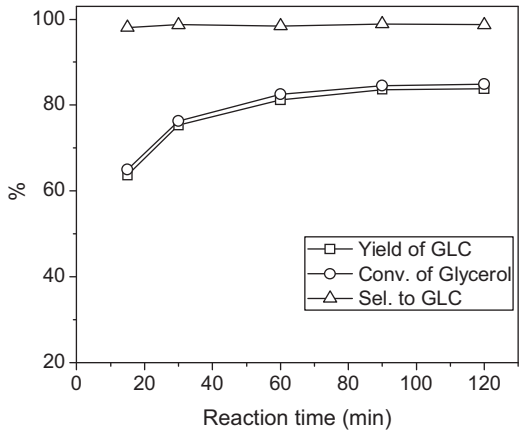

Fig. 11. Effect of reaction time on the transesterification of DMC with glycerol. Reaction condition: DMC/glycerol = 2, catalyst/glycerol = 5 wt%, T = 90 °C.

concentration increased proportionally, consistent with the catalytic activity of MgO–S series. When the surfactant/Mg precursor weight ratio was higher than 5, the catalysts showed similar catalytic activity as well as similar basic site concentration.

The shapes of the catalysts were also affected by the amount of surfactant. Fig. 10 reveals that MgO–S(5) has a uniform sphere-like particle shape, while MgO–S(0.5) shows some agglomeration of spherical particles. Further decrease of the amount of surfactant caused the spherical particles to disappear, as observed for MgO–S(0.2). On the other hand, as shown in Table S3 in Supporting information, the amount of surfactant did not affect the surface area, as expected. Additionally, based on an elemental analysis, the amount of carbon remaining in MgO was negligible, indicating almost all of surfactant was decomposed during calcination.

3.4. Effect of reaction conditions

The effect of reaction time on the transesterification of DMC with glycerol was investigated using MgO–S(5) in a range of 15–120 min at 90 °C with a DMC/glycerol molar ratio of 2 and a catalyst to glycerol ratio of 5 wt%. As can be seen in Fig. 11, the yield of GLC significantly increased as the reaction time was increased from 15 to 60 min. Further increase of the reaction time over 90 min led to a similar yield of GLC, indicating that the reaction reached equilibrium within 90 min.

The effect of the DMC/glycerol ratio was also investigated and the results are shown in Fig. 12. An increase of the DMC/glycerol molar ratio from 1 to 4 increased the yield of GLC from 61.0% to 76.5%. Further increase of the DMC amount led to a decrease of the yield and selectivity of GLC. It appears that the increase of DMC concentration in the reaction solution generates side products such as diglycerol tricarbonate from the secondary reactions of GLC with DMC or glycerol [26].

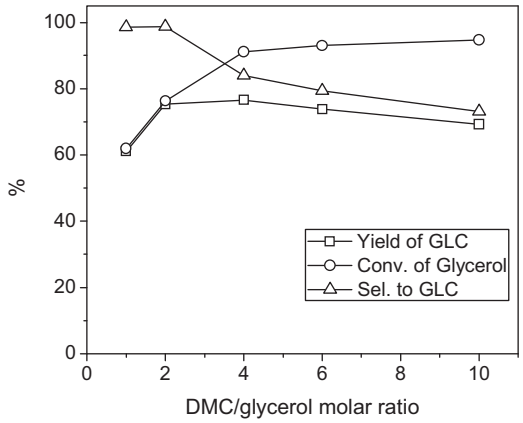

Fig. 12. Effect of DMC/glycerol molar ratio on the transesterification of DMC with glycerol. Reaction condition: Catalyst/glycerol = 5 wt%, T = 90 °C, t = 30 min.

3.5. Reusability

We investigated the reusability of the catalyst using MgO–S(5). After the reaction, the catalyst was centrifuged and directly reused for the next reaction. The results shown in Fig. S2 reveal that the yield of GLC decreased from 83.6 to 65.8% at the first reuse. The yields of GLC continuously decreased to 43.8 and 39.3% at the 3rd and 5th reuse, respectively, but the selectivities were maintained at 96%. The decrease of the catalytic activity is likely caused by deactivation of the catalyst due to the presence of glycerol carbonate remaining on the surface of the catalyst as shown by the FT-IR analysis results in Fig. S3. To remove glycerol carbonate residue, the catalyst was heated to 400 °C in a nitrogen atmosphere and

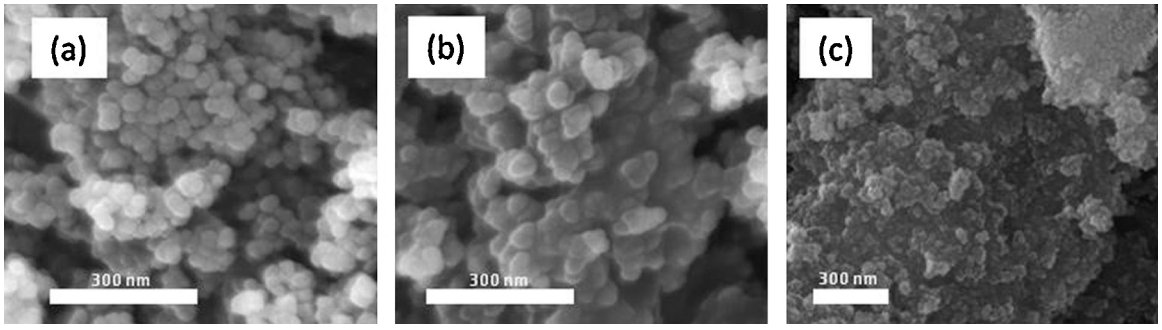

Fig. 10. SEM images of (a) MgO–S(5), (b) MgO–S(0.5), and (c) MgO–S(0.2).

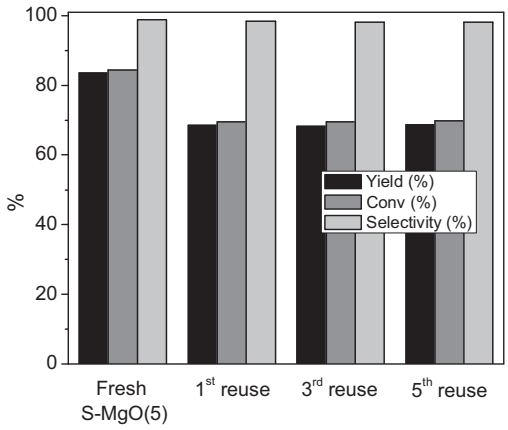

Fig. 13. Reuse of MgO–S(5) after calcination at 500 °C in air. Reaction condition: DMC/glycerol = 2, catalyst/glycerol = 5 wt%, T = 90 °C, t = 90 min.

subsequently calcined at 500 °C in air for 2 h. In spite of the calcination, the catalytic activity decreased to 68.6%, however, as shown in Fig. 13, the activity was maintained at this level by the calcination after use. Further increase of calcination temperature to 680 °C did not result in an increase of the GLC yield.

The effect of calcination after use of the catalyst MgO–S on the catalyst morphology was investigated using XRD. As can be seen from Figs. S4 and S5 in the Supporting information, there were no significant change to the crystallite size and crystal phase after reuse and calcinations. However, after the 3rd and 5th reuse, the surface area decreased to 40 and 34 m^2/g, respectively (see Table S4), due to agglomeration in some parts of the catalyst, as observed in the SEM images (see Fig. S6).

4. Conclusion

The preparation method of magnesium oxides resulted in different morphologies of magnesium oxides as well as different catalyst activity in the synthesis of glycerol carbonate from glycerol and dimethyl carbonate. MgO prepared by the precipitation method had the highest surface area but showed poor catalytic activity. In contrast, MgO prepared using the surfactant pluronic F127, which had only half the surface area of MgO prepared by the precipitation method, showed much higher catalytic activity. It is assumed that the surfactant plays a role of creating low coordination O^{2-} sites on the surface of MgO, thereby increasing the basicity and basic site concentration. By increasing the amount of the surfactant with respect to the magnesium precursor, the basic site and catalytic activity increased linearly until a surfactant/Mg precursor weight ratio of 5, and they remained constant beyond that level. Although direct catalyst reuse after the reaction resulted in poor product yield, with calcination of the used catalyst at 500 °C, the catalytic activity was restored to 90% of that obtained with the fresh catalyst.

Acknowledgments

This work was supported by 'Eco-process based technologies' grant funded by Korea Ministry of Environment. This work was also supported by 'Creative Allied Project (CAP)' grant funded by the Korea Research Council of Fundamental Science and Technology (DRCF) and KIST institutional program (Project No. 2E24832).

Appendix A. Supplementary data

Supplementary data associated with this article can be found, in the online version, at http://dx.doi.org/10.1016/j.apcata.2014.06.028.

References

[1] H. Tsuji, F. Yagi, H. Hattori, H. Kita, J. Catal. 148 (1994) 759–770.
[2] H.H. Huang, W.C. Shih, C.H. Lai, Appl. Phys. Lett. 96 (2010) 193505.
[3] F. Laoutid, L. Ferry, J.M. Lopez-Cuesta, A. Crespy, Fire Mater. 30 (2006) 343–358.
[4] Z. Zhou, S. Xie, D. Wan, D. Liu, Y. Gao, X. Yan, H. Yuan, J. Wang, L. Song, L. Liu, W. Zhou, Y. Wang, H. Chen, J. Li, Solid State Commun. 131 (2004) 485–488.
[5] X. Li, W. Xiao, G. He, W. Zheng, N. Yu, M. Tan, Colloids Surf., A: Physicochem. Eng. Aspects 408 (2012) 79–86.
[6] I.V. Mishakov, A.F. Bedilo, R.M. Richards, V.V. Chesnokov, A.M. Volodin, V.I. Zaikovskii, R.A. Buyanov, K.J. Klabunde, J. Catal. 206 (2002) 40–48.
[7] V.V. Chesnokov, A.F. Bedilo, D.S. Heroux, I.V. Mishakov, K.J. Klabunde, J. Catal. 218 (2003) 438–446.
[8] B.Q. Xu, J.M. Wei, H.Y. Wang, K.Q. Sun, Q.M. Zhu, Catal. Today 68 (2001) 217–225.
[9] M. Verziu, B. Cojocaru, J. Hu, R. Richards, C. Ciuculescu, P. Filip, V.I. Parvulescu, Green Chem. 10 (2008) 373.
[10] Y. Ding, G. Zhang, H. Wu, N. Hai, L. Wang, Y. Qian, Chem. Mater. 13 (2001) 435.
[11] S.W. Bian, J. Baltrusaitis, P. Galhotra, V.H. Grassian, J. Mater. Chem. 20 (2010) 8705–8710.
[12] C.M. Janet, B. Viswanathan, R.P. Viswanath, T.K. Varadarajan, J. Phys. Chem. C111 (2007) 10267–10272.
[13] K.T. Ranjit, K.J. Klabunde, Chem. Mater. 17 (2005) 65–73.
[14] S. Utamapanya, K.J. Klabunde, J.R. Schlup, Chem. Mater. 3 (1991) 175–181.
[15] Y. Yin, G. Zhang, Y. Xia, Adv. Funct. Mater. 12 (2002) 293–298.
[16] R. Richards, W. Li, S. Decker, C. Davidson, O. Koper, V. Zaikovski, A. Volodin, T. Rieker, K.J. Klabunde, J. Am. Chem. Soc. 122 (2000) 4921–4925.
[17] W.-C. Li, A.-H. Lu, C. Weidenthaler, F. Schüth, Chem. Mater. 16 (2004) 5676–5681.
[18] J. Zhou, S. Yang, J. Yu, Colloids Surf., A: Physicochem. Eng. Aspects 379 (2011) 102–108.
[19] Z. Zhao, H. Dai, Y. Du, J. Deng, L. Zhang, F. Shi, Mater. Chem. Phys. 128 (2011) 348–356.
[20] W. Wang, X. Qiao, J. Chen, H. Li, Mater. Lett. 61 (2007) 3218–3220.
[21] H. Jeon, D.J. Kim, S.J. Kim, J.H. Kim, Fuel Process. Technol. 116 (2013) 325–331.
[22] A. Ganguly, P. Trinh, K.V. Ramanujachary, T. Ahmad, A. Mugweru, K.A. Ganguli, J. Colloid Interface Sci. 353 (2011) 137–142.
[23] Huntsman Corporation, JEFFSOL® Glycerine Carbonate, Huntsman Corporation, 2009, http://www.huntsman.com/performance_products/Media/JEFFSOL%20Glycerine%20Carbonate.pdf.
[24] D. Randall, R. De Vos, Eur. Patent EP 419114, 1991.
[25] M. Weuthen, U. Hees, Ger. Patent DE 4335947, 1995.
[26] G. Rokicki, P. Rakoczy, P. Parzuchowski, M. Sobiecki, Green Chem. 7 (2005) 529–539.
[27] L. Ubaghs, N. Fricke, H. Keul, H. Hocker, Macromol. Rapid Commun. 25 (2004) 517–521.
[28] A. Takagaki, K. Iwatani, S. Nishimura, K. Ebitani, Green Chem. 12 (2010) 578–581.
[29] F.S.H. Simanjuntak, V.T. Tanda, C.S. Kim, B.S. Ahn, Y.J. Kim, H. Lee, Chem. Eng. Sci. 94 (2013) 265–270.
[30] M. Malyaadri, K. Jagadeeswaraiah, P.S. Sai Prasad, N. Lingaiah, Appl. Catal., A: Gen. 401 (2011) 153–157.
[31] T. Selvamani, A. Sinhamahapatra, D. Bhattacharjya, I. Mukhopadhyay, Mater. Chem. Phys. 129 (2011) 853–861.
[32] S. Stankic, M. Muller, O. Diwald, M. Sterrer, E.J. Bernardi, Angew. Chem. Int. Ed. 44 (2005) 4917–4920.
[33] M. Sterrer, T. Berger, O. Diwald, E. Knözinger, J. Am. Chem. Soc. 125 (2003) 195–199.
[34] J.R. Ochoa-Gomez, O. Gomez-Jimenez-Aberasturi, B. Maestro-Madurga, A. Pesquera-Rodriguez, C. Ramirez-Lopez, L. Lorenzo-Ibarreta, J. Torrecilla-Soria, M.C. Villaran-Velasco, Appl. Catal., A: Gen. 366 (2009) 315–324.